Evolution of Developmental Control Mechanisms

Wnt signaling underlies evolution and development of the butterfly wing pattern symmetry systems

Arnaud Martin [a,b,*], Robert D. Reed [a]

[a] *Department of Ecology and Evolutionary Biology, Cornell University, Ithaca, NY 14853, USA*
[b] *Department of Developmental and Cellular Biology, Irvine, CA 92697, USA*

ABSTRACT

Most butterfly wing patterns are proposed to be derived from a set of conserved pattern elements known as symmetry systems. Symmetry systems are so-named because they are often associated with parallel color stripes mirrored around linear organizing centers that run between the anterior and posterior wing margins. Even though the symmetry systems are the most prominent and diverse wing pattern elements, their study has been confounded by a lack of knowledge regarding the molecular basis of their development, as well as the difficulty of drawing pattern homologies across species with highly derived wing patterns. Here we present the first molecular characterization of symmetry system development by showing that *WntA* expression is consistently associated with the major basal, discal, central, and external symmetry system patterns of nymphalid butterflies. Pharmacological manipulations of signaling gradients using heparin and dextran sulfate showed that pattern organizing centers correspond precisely with *WntA*, *wingless*, *Wnt6*, and *Wnt10* expression patterns, thus suggesting a role for *Wnt* signaling in color pattern induction. Importantly, this model is supported by recent genetic and population genomic work identifying *WntA* as the causative locus underlying wing pattern variation within several butterfly species. By comparing the expression of *WntA* between nymphalid butterflies representing a range of prototypical symmetry systems, slightly deviated symmetry systems, and highly derived wing patterns, we were able to infer symmetry system homologies in several challenging cases. Our work illustrates how highly divergent morphologies can be derived from modifications to a common ground plan across both micro- and macro-evolutionary time scales.

© 2014 Elsevier Inc. All rights reserved.

Introduction

Butterfly wing patterns are a crucible of morphological diversity that provide an ideal template to study the mechanisms that drive pattern evolution (Beldade and Brakefield, 2002; Joron et al., 2006; Nijhout, 1991). Several recent studies have narrowed down the genetic basis of wing pattern variation to single genes, explaining phenotypic switches involved in adaptive mimicry and sexual selection (Gallant et al., 2014; Joron et al., 2011; Kunte et al., 2014; Martin et al., 2012; Reed et al., 2011). Importantly, some of these mechanisms of intraspecific variation also appear to act at deeper taxonomic scales, with the same genes repeatedly causing similar trait differences in convergent lineages (Gallant et al., 2014; Martin and Orgogozo, 2013; Martin et al., 2012; Papa et al., 2008; Reed et al., 2011). Butterfly wing patterns thus combine several unique properties for understanding developmental evolution by offering the potential to study the genetic basis of phenotypic variation between populations, including in the context of adaptation; to tackle the problem of developmental evolution in a relatively simple, two-dimensional field of cells; and to test the extension of these evolutionary developmental mechanisms at a range of taxonomic scales. The promise of using wing patterns to bridge the gap between micro- and macro-evolutionary times scales, however, rests largely on our ability to determine the developmental homologies of pattern elements between divergent species.

In 1924, Schwanwitsch presented a schema for a "prototype" butterfly wing pattern, which, he argued, represented a basic set of conserved pattern elements that had been repeatedly modified by evolution to produce most of the color pattern diversity we see in nature (Nijhout, 1991; Schwanwitsch, 1924). This schema, which is now commonly referred to as the *nymphalid ground plan*, provides a formal nomenclature for wing pattern elements seen in butterflies and moths, and has served as a foundation for rapidly growing literature on wing pattern evolution (Nijhout, 1991; Schwanwitsch, 1924, 1956; Otaki, 2012; Süffert, 1927). In order, along the proximo-distal axis, keeping most of the nomenclature
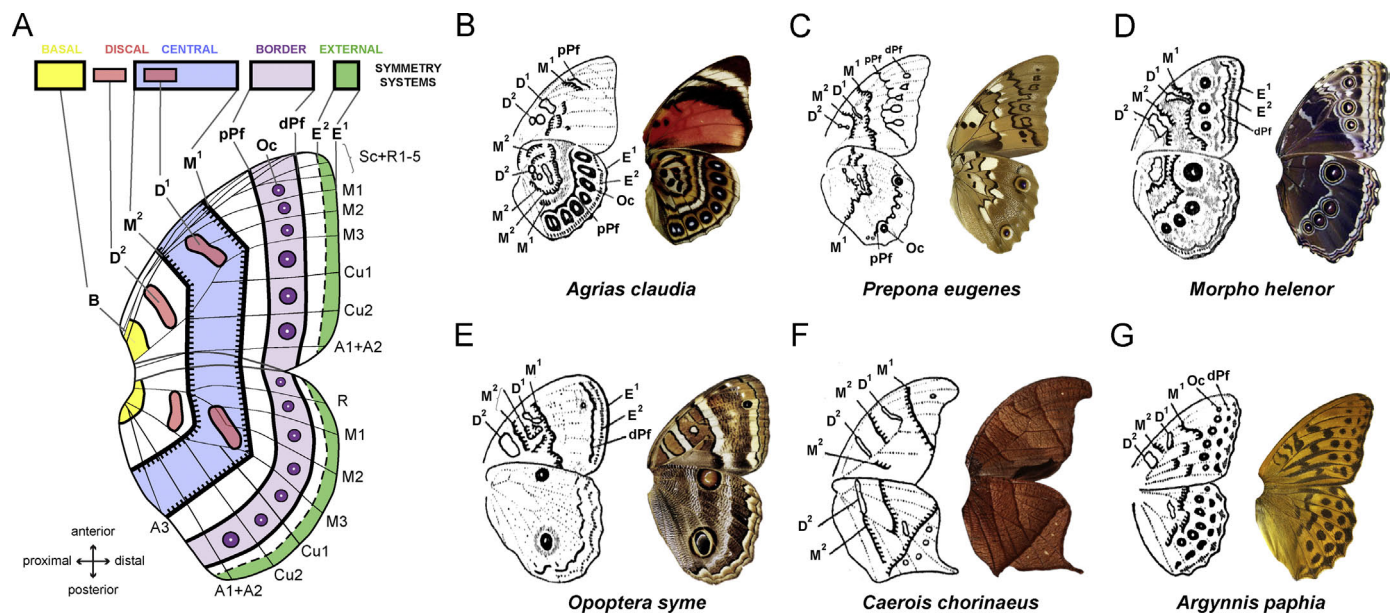
Fig. 1. The symmetry systems of the nymphalid ground plan and their diversification. (A) Schematic of the nymphalid ground plan. (B–G) Examples of derivations of the nymphalid ground plan; drawings are reproduced from Schwanwitsch (1956) with adapted annotations and representative photographs of the corresponding species. See text for legend.

of Schwanwitsch (1956), the major elements of the nymphalid ground plan are as follows (Fig. 1A and B):

(1) Basalis (B, *syn.* Root band), a symmetry system for which only the distal half is usually visible.
(2) Discalis II (D^2), a small pattern delimited on the antero-posterior axis by the veins of the discal cell. *wingless* (*wg, syn. Wnt1*) expression marks this pattern (Martin and Reed, 2010).
(3) Discalis I (D^1, *syn.* Discal spot), which is always centered on the discal crossvein and can be easily identified across a wide range of lepidopterans. Like in D^2, the antero-posterior domain of D^1 is delimited by the veins of the discal cells. When present, D^1 and D^2 have similar color compositions, both express *wg*, and can be considered serial homologs (Martin and Reed, 2010). For this reason, we maintain here the original Discalis terminology from Schwanwitsch, and avoid the proposal of Otaki to treat D^2 as an independent pattern system (Otaki, 2012). Nijhout has proposed that both D^1 and D^2 may be small-scale symmetry systems in themselves (Nijhout, 1991; Nijhout and Wray, 1988).
(4) The central symmetry system, delimited by the proximal (M^2) and distal (M^1) bands. In Nymphalidae, M^2 is rarely complete and is often limited to the discal cell, while M^1 can usually be seen as an arc or straight line spanning between the anterior and posterior wing margins (Nijhout, 1994).
(5) The border ocelli (Oc, often called eyespots), which take the form of individuated circular patterns centered between veins. When present, border ocelli can range from simple dots to complex concentric rings of color fields, and often show radial symmetry around a focal point. These patterns have been well studied from both a developmental and evolutionary perspective, and a number of candidate genes have been implicated in eyespot patterning (Beldade and Saenko, 2009; Brunetti et al., 2001; Oliver et al., 2012; Reed and Serfas, 2004; Saenko et al., 2011). Grafting experiments have shown that these patterns are organized by the focal expression of inductive signals (Monteiro et al., 2001; Nijhout, 1980).
(6) The proximal and distal parafocal elements (pPf and dPf) are a system of patterns that frame the Oc patterns, although they can also be observed in the absence of Oc elements. These parafocal patterns were associated to the border symmetry system in a recent update of the nymphalid ground plan (Otaki, 2012), while Schwanwitsch did not consider pPf (variably called external or ocellar Umbra) or dPf (formerly called E^3) as part the same symmetry system.
(7) The marginal Externae patterns (E^2 and E^1) that border the distal edge of the wing.

Other pattern systems such as the intervenous, venous, and ripple patterns have been discussed elsewhere but do not indicate positional homologies between species (Nijhout, 1978).

The largest, and often the most prominent, pattern elements of the ground plan are a set of stripe-based patterns which Süffert dubbed the *symmetriesystems* (Nijhout, 1994; Otaki, 2012; Süffert, 1927, 1929), due to the fact that in many species they are composed of systems of parallel lines of pigmentation that mirror each other along linear organizing centers (Fig. 1A). The central symmetry system, defined by its boundary elements M^1 and M^2, is arguably the largest and most diverse wing pattern feature in butterflies, however it is also the most challenging to reliably identify in many species (examples in Fig. 1B–H). Unfortunately, work on the symmetry systems has been largely confounded by two related limitations. First, no clear markers or candidate genes have thus far been identified to allow investigations into the molecular basis of symmetry system development. Although there is experimental evidence for long-range induction of symmetry system color patterns (Nijhout, 1994, 1978, 1985; Monteiro et al., 2001; Toussaint and French, 1988; Otaki, 2011), no specific molecules have yet been associated with the determination or induction of these patterns. Second, it is very difficult to determine to what extent the wing patterns of highly derived species are associated with, or derived from, specific symmetry systems. In some species it is straightforward to assign color patterns to specific symmetry systems, however in many other species, including important models like *Heliconius*, it is difficult or impossible to confidently identify developmental homologies of pattern elements. Because the symmetry systems appear to underlie the majority of wing pattern diversity in Lepidoptera, the lack of advancement in understanding how these patterns develop and evolve has been a major frustration for those working on butterfly wing patterns.

When considering candidate molecules for symmetry system development, our attention was drawn to the *Wnt* family of signaling ligands for a combination of several reasons: (1) Grafting, ablation, and pharmacological manipulations have all indicated that short- or long-range induction is involved in determining symmetry system color pattern in some moths and butterfly (Monteiro et al., 2001; Toussaint and French, 1988; Serfas and Carroll, 2005). As well, the alternating patterns of color stripes are consistent with a morphogen gradient-like process (Nijhout, 1978, 2001). Wnt signaling is well known for both of these characteristics. (2) *wg* (*Wnt1*) expression is associated with determination of the D^1 and D^2 spots, which have been proposed to be small-scale symmetry systems (Carroll et al., 1994; Martin and Reed, 2010; Otaki, 2012). (3) In *Heliconius*, *WntA* expression boundaries in the larval wing disk delineate the future contours of the forewing light-colored fields of all species and morphs that have been examined (Martin et al., 2012). While *Heliconius* wing patterns are highly derived and difficult to relate to the nymphalid ground plan, it has been speculated that these patterns may be associated with the M^1 and M^2 bands even though there are no observable symmetry patterns (Nijhout and Wray, 1988). (4) *WntA* expression also marks the proximal contour of the white band in *Limenitis arthemis* (Gallant et al., 2014), consistent with previous predictions that M^1 corresponds to the proximal boundary of similar white fields in nymphalid butterflies (Nijhout, 1991; Otaki, 2012). As in *Heliconius*, however the symmetric organization of ground plan patterns is not visible in the derived patterns of *Limenitis*, making it difficult to determine to what extent *Limenitis* patterns might be derived from the central symmetry system. (5) Independent genetic mapping and SNP association studies have identified the *WntA* locus as causing wing pattern variation in five different butterfly species: *L. arthemis* (Gallant et al., 2014), *Heliconius melpomene* (Martin et al., 2012), *Heliconius cydno* (Gallant et al., 2014; Martin et al., 2012), and *Heliconius erato* and its sister species *Heliconius himera* (Martin et al., 2012; Nadeau et al., 2014; Papa et al., 2013). In all of these cases, allelic variation of *WntA* determines the phenotypes of the *WntA*-positive color pattern elements described above. It follows that the *WntA* locus itself has driven color pattern evolution several times. Despite this, however, due to the derived nature of *Heliconius* and *Limenitis* wing patterns, it is still unclear how, or if, *WntA* patterns relate to the nymphalid ground plan.

Here we examine the expression of *WntA* and other Wnt-family genes in butterflies displaying different degrees of deviation from the nymphalid ground plan. Our comparative results suggest that the composite regulation of the Wnt signals has been a key determinant of pattern formation and evolution. Not only do these data dramatically improve our understanding of the developmental nature of symmetry systems in butterflies, they also validate the hypothesis, derived from intra-specific studies, that regulatory evolution of *WntA* has driven major pattern shifts at many phylogenetic levels within Nymphalidae.

Material and methods

Animals

Fifth instar larvae of *Euphydryas chalcedona* were collected on *Keckiella cordifolia* plants in April–May 2013 in the vicinity of Morris Reservoir (Azusa, CA). Fifth instar larvae of *Agraulis vanillae* were collected on *Passiflora caerulea* plants in August–October 2012 and 2013 around the Huntington Beach Central Library (Huntington Beach, CA). *Vanessa cardui* larvae were obtained from a commercial provider and reared on artificial medium (Carolina Biological Supplies, Burlington, NC, USA). *Junonia coenia* larvae

originated from a laboratory colony maintained at Cornell University (RDR), which derives from the North Carolina laboratory stock maintained by Laura Grunert and Fred Nijhout (Duke University, NC, USA).

Gene cloning

Fifth instar wing disks from each species were dissected in ice cold PBS, stored in TRIzol® Reagent (Life Technologies, Grand Island, NY, USA). Total RNA was extracted from tissue lysates using the Direct-zol RNA miniprep kit (Zymo Research, Irvine, CA, USA), and used as a template for reverse transcription with the iScript cDNA Synthesis kit (BioRad, Hercules, CA, USA). PCR amplification of Wnt genes was performed using degenerate primers, followed by TA-cloning and verification of correct insertion by sequencing (Supplementary Table 1). The resulting plasmids were used for DIG-labeled riboprobe synthesis following manufacturer's recommendations (Roche Applied Science, Indianapolis, IN, USA).

Wing disk whole-mount in situ hybridization

Fifth instar larvae were cold-anaesthetized, dissected in PBS, immediately transferred to 1.5 mL tubes containing fixative (formaldehyde 9% in PBS containing 50 mM ethylene glycol tetraacetic acid) for 30 min on ice, washed five times with PBST (PBS, 0.01% Tween 20), gradually dehydrated in increasing concentrations of MeOH (33% and 66% in PBS) and stored at −20 °C in MeOH (100%) for up to one year. For in situ hybridization, following rehydration and washes in PBST, wing disks were incubated 5 min with 25 µg/mL proteinase K in cold PBST, washed in cold PBST containing 2 mg/mL glycine, and washed in cold PBST. After this step, periopodial membranes were removed from the surface of the wing disks using fine forceps, followed by a post-fixation 20 min on ice in PBS containing 5.5% formaldehyde, washes in cold PBST, gradual transfer to a standard hybridization buffer (5× saline sodium citrate pH 4.5, 50% formamide, 0.01% Tween20, 100 µg/mL denatured salmon sperm DNA, final pH 5–6 at 22 °C), pre-incubation at 62–65 °C for an hour, and incubation in hybridization buffer supplemented with 1 g/L glycine and 30 ng/mL riboprobe for 16–40 h at 63 °C. Upon completion of the hybridization step, wing disks were washed eight times 15–30 min in hybridization buffer, returned to room temperature, and gradually stepped back into PBST. For secondary detection of the riboprobe, the tissues were washed on PBST, blocked for 30 min in Tris buffer saline, 0.01% Tween20 (TBST, pH=7.5) supplemented with 1 g/L bovine serum albumin, incubated with a 1:3000 dilution of anti-digoxigenin alkaline phosphatase Fab fragments (Roche Applied Science), washed ten times (10–120 min per wash) in cold TBST, incubated in an alkaline phosphatase buffer (100 mM Tris–HCl pH 9.5, 100 mM NaCl, 5 mM MgCl2, 0.01% Tween20), and finally stained with BM Purple (Roche Applied Science) for 4–8 h at room temperature. Stained tissues were then washed in PBST 2 mM ethylene diamine tetraacetic acid and slide mounted in PBS containing 60% glycerol, and photographed with a Nikon Coolpix P5100 digital camera (Nikon Inc. USA, Melville, NY, USA) mounted with a LNS-30D/P51 adapter (Zarf Enterprises, Spokane, WA, USA) on a Leica MZFLII stereomicroscope (Leica Microsystems, Buffalo Grove, IL, USA). Ventral and dorsal expression patterns matched perfectly, and only dorsal views are shown here. Developmental stages of wing discs were categorized according to Reed et al. (2007).

Injections

Pupal injections of heparin and dextran sulfate were performed following a previously published procedure (Serfas and Carroll, 2005), with the exception that glass capillary needles mounted on a micro-injector were used instead of a micro-syringe. Pupae

reared at room temperature (24–25 °C) were injected 10–16 h after pupation into the left wing pouch without direct contact with wing tissue, in a space situated near the baso-posterior edge of the forewing. Heparin and dextran sulfate injections result in systemic effects that affect both the injected and non-injected wings (Serfas and Carroll, 2005), and the abdomen can be injected instead of the wing pouch with similar efficiency.

Results

Expression of Wnt-family genes in the prototypical ground plan

To gain insight into the regulatory landscape of the nymphalid ground plan, we characterized the expression of *WntA* and other *Wnt*-family genes in wing disks from last-instar larvae of *E. chalcedona* (Fig. 2). The ventral wing surfaces of this butterfly are an excellent model for the prototypical nymphalid ground plan because all the ground plan elements (B, D^1, D^2, M^{1-2}, pPf–Oc–dPf, E^{1-2}) can be readily identified, and both the basal and central symmetry systems show clear symmetry on the ventral hindwing. *WntA* expression revealed a spatially restricted pattern divided in three elongated domains: (1) a basal stripe of weak expression, more marked in hindwings than in forewings, that appears to be correlated with B patterns. (2) A median stripe of expression overlapping with the crossvein and showing local protrusions extending distally. A closer look at the ventral hindwing (more amenable to interpretation than other wing surfaces in this butterfly) shows that median *WntA* expression precisely delineates the presumptive domain of the central orange with black outline stripe (M^1 and M^2, and overlap with D^1). (3) An external complex of chevron-like patterns, marking the presumptive E^{1-2} patterns. As expected from previous work (Carroll et al., 1994; Macdonald et al., 2010; Martin and Reed, 2010), *wg* marked the D^1 and D^2 elements as well as the wing peripheral tissue. *Wnt6* and *Wnt10* showed similar expression in the peripheral tissue and discal symmetry systems, with the exception that we did not detect *Wnt10* in the hindwing D patterns. Of note, *wg*/*Wnt6*/*Wnt10* form a cluster of consecutive duplicated genes that is highly conserved across arthropod genomes (Bolognesi et al., 2008; Janssen et al., 2010) and is observed in the current genome assemblies of two butterflies (Heliconius Genome Consortium, 2012; Zhan and Reppert, 2013). The similarity of *wg*/*Wnt6*/*Wnt10* expression patterns is consistent with previous reports of functional and regulatory redundancy between these three ancient paralogues in several organisms and tissues (Gieseler et al., 2001; Hogvall et al., 2014; Janson et al., 2001; Janssen et al., 2010), and suggests the existence of shared regulatory elements that coordinate their expression in wing disks. The remaining Wnt genes that have been detected in nymphalid butterfly genomes – *Wnt5*, *Wnt7*, and *Wnt9* (Martin et al., 2012; Zhan and Reppert, 2013) – could not be amplified from wing disk cDNA (Supplementary Table 1).

In summary, expression of Wnt genes marks the development of the basal (*WntA*), discal (*wg*/*Wnt6*/*Wnt10*), central (*WntA*), and external (*WntA*) symmetry systems of *E. chalcedona*. In addition, all these patterns show similar color compositions and symmetries – orange with black outlines – suggesting that different Wnt ligands converge on similar phenotypic outputs in a representative of the prototypical nymphalid ground plan.

Co-regulation of the basal, discal, central, and external symmetry systems by the Wnt pathway

If ligands of the same pathway specify the different symmetry systems, one would predict that manipulation of the pathway should produce co-varying effects on the basal, discal, central, and external symmetry systems. To test this we carried out some simple pharmacological assays using heparin and dextran sulfate in *E. chalcedona*. Functional work in model organisms has shown that heparin binds extracellular Wnt ligands and positively enhances their secretion, stability, and transport (Baeg et al., 2001; Binari et al., 1997; Bradley and Brown, 1990; Fuerer et al., 2010; Greco et al., 2001; Hufnagel et al., 2006; Reichsman et al., 1996), suggesting a model where the heparin-like sugar chains of endogenous proteoglycans are critical to Wnt movement and shape its extracellular distribution gradient (Lin, 2004; Yan and Lin, 2009). Based on this, heparin would be expected to induce Wnt gain-of-function effects, and indeed, heparin injections in various butterflies have supported this prediction. Serfas and Carroll previously noted that heparin injections in *J. coenia* result in expansion of the basal, discal and external symmetry systems (Serfas and Carroll, 2005), precisely corresponding with *wg* expression domains in the D^2 and D^1 elements (Martin and Reed, 2010; Serfas and Carroll, 2005). As well, heparin injections in *Limenitis* and *Heliconius* phenocopy the effects of *WntA* allelic variants in these genera (Martin et al., 2012; Gallant et al., 2014). As in this previous work, we found that injection of heparin into *E. chalcedona* pupae produced effects consistent with Wnt gain-of-function (Fig. 3A–C). This effect was particularly prominent on the ventral hindwing, where the basal, discal, and central symmetry systems showed the most extreme dilations. The black outline of the *Wnt*-positive external symmetry system (E^2) also expanded. In contrast, the *Wnt*-negative border symmetry system (pPf–Oc–dPf) faded upon heparin injection, an effect that was also previously observed in *J. coenia* (Serfas and Carroll, 2005).

Like heparin, dextran sulfate is a sulfated polysaccharide, however it has been shown to inhibit an endogenous proteoglycan in mice – an effect reversed by heparin (Floer et al., 2010). Although the specific mechanism of dextran sulfate's inhibitory effect is unknown, injections in *J. coenia* result in very specific diminution of symmetry systems elements, including *wg*-positive D^1 and D^2 elements (Serfas and Carroll, 2005). We thus speculate that dextran sulfate acts as an inhibitor of endogenous heparin-like proteoglycans involved in Wnt signaling. Accordingly, as in *J. coenia*, dextran sulfate injections in *E. chalcedona* had the opposite effects of heparin injections, and resulted in marked contractions of all *Wnt*-positive color patterns (B, D^2, D^1, M^{1-2}, E^{1-2}) and moderate expansions of *Wnt*-negative patterns. Thus, while a functional connection between dextran sulfate injections and Wnt signaling is only speculative at this point, the injections nonetheless demonstrate co-variation of multiple patterns that are specifically correlated with *Wnt* expression.

We must note the important caveat that a direct link between Wnt signaling and the injection treatments cannot yet be irrefutably demonstrated. We observed *Wnt* mRNA expression prior to pupation, yet injected heparin shortly after pupation at a stage when we hypothesize Wnt proteins are functioning as signaling ligands. Unfortunately, with current tools in our system it is difficult to directly visualize Wnt protein distribution, or test Wnt ligand interactions with heparin. This said, heparin can at least reveal which patterns are co-regulated by extracellular signals in a given species. This, coupled with *Wnt*-family gene expression in *E. chalcedona*, does indicate that the basal, discal, central, and external symmetry systems are co-regulated by similar signals. We thus propose a model of wing patterning where various sources of Wnt-molecules collectively contribute to the specification of orange and black symmetry system patterns along the proximo-distal axis of the checkerspot wing (Fig. 3D). *WntA* in particular emerges as a key player in this multiple-source system. In order to gain further insight into the evolution and development of central symmetry patterns, we focus our attention on *WntA* in the rest of the study.
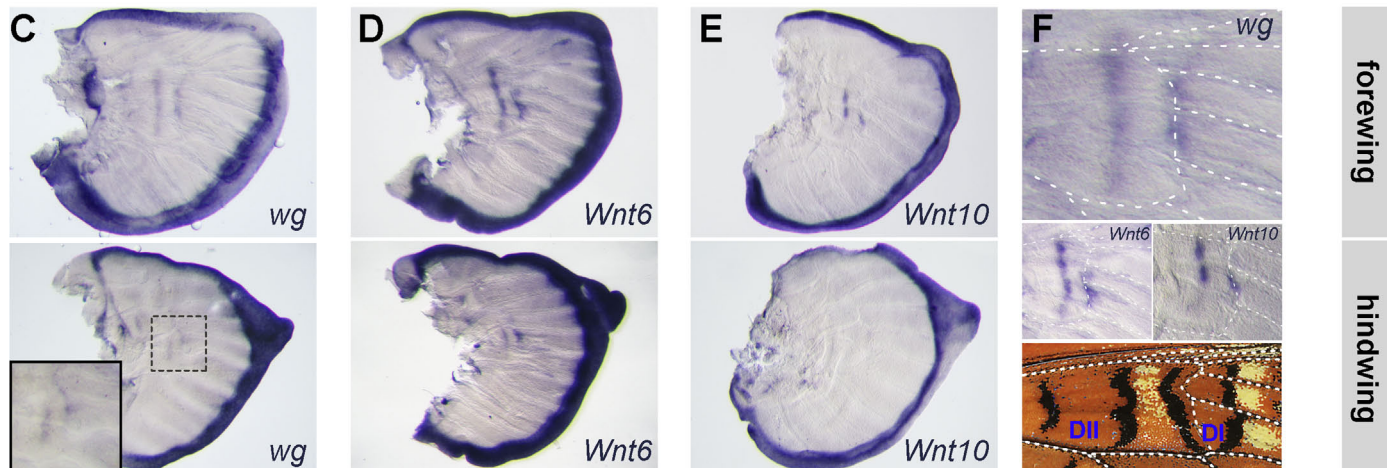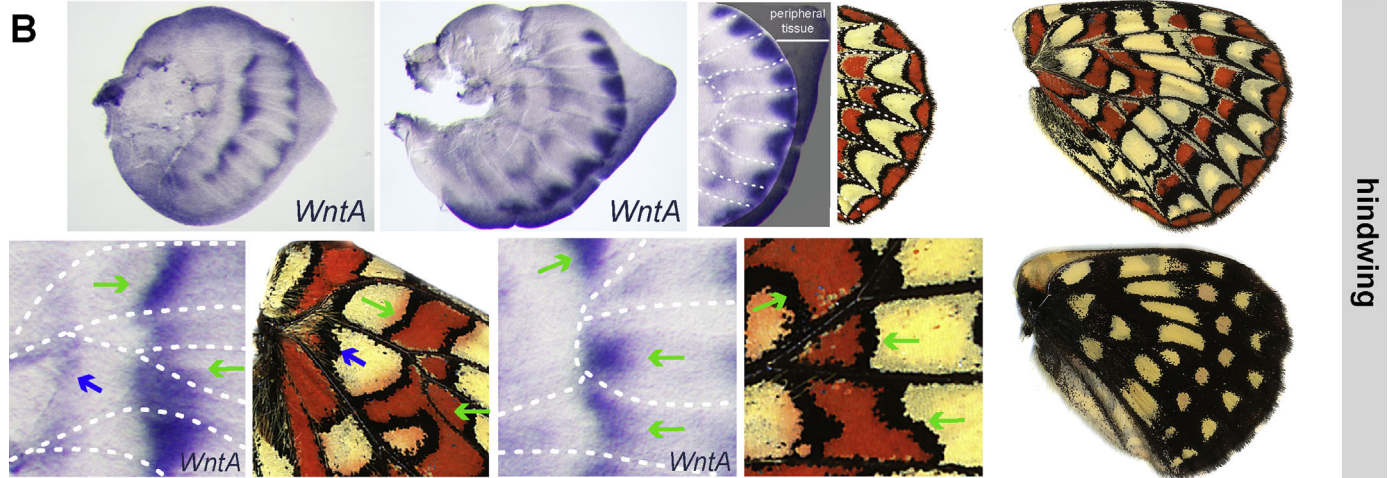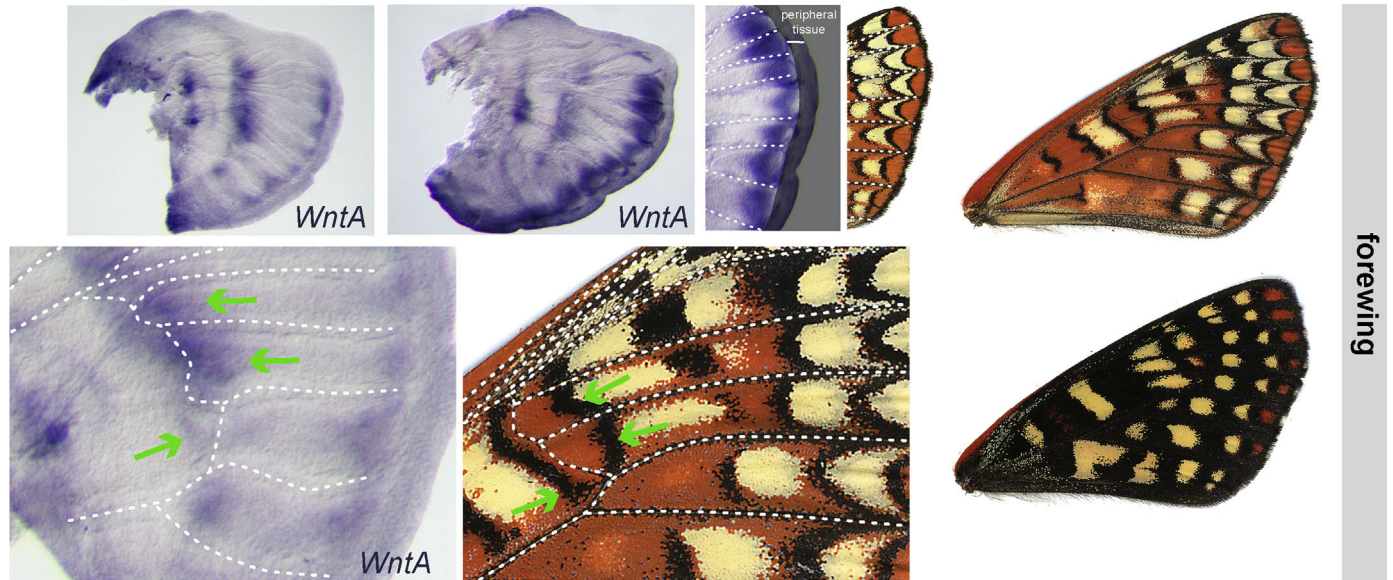
Fig. 2. Expression of *Wnt* ligand genes in *E. chalcedona* symmetry systems. (A) Expression of *WntA* in the larval forewing disks of *E. chalcedona*, shown at two successive stages (top panels; left: Stage 2.0; right: Stage 3.0). The vein system of larval wing disks prefigures the adult veins (dotted white lines). Marginal expression in intervenous chevrons corresponds to orange patterns of the external symmetry system. Central expression overlaps with the presumptive D^1 discal symmetry system (green arrows) and extends distally and posteriorly, in association with the presumptive organizing center of the central symmetry system. Note that the peripheral tissue along larval wing disk margins undergoes apoptosis in the pupa and is not represented in adult wings (Dohrmann and Nijhout, 1988; Macdonald et al., 2010). (B) Expression of *WntA* in the larval hindwing disks of *E. chalcedona*, shown at two successive stages (top panels, from left to right: Stage 1.75; Stage 3.0). *WntA* precisely outlines the presumptive orange patterns of the external, basal (blue arrow), and central symmetry systems (green arrows). (C–E) Expression of the genes of the *wg/Wnt6/Wnt10* complex mark the wing peripheral tissue and the D^2 and D^1 discal symmetry systems. *Wnt10* was not detected in the hindwing discal patterns. C, forewing: Stage 2.5; C, hindwing: Stage 1.5; D, forewing: Stage 2.5; D, hindwing: Stage 1.75; E, forewing: Stage 2.0; Stage 2.0 (F) Magnified view of *wg/Wnt6/Wnt10* expression in the presumptive forewing D^2 and D^1 discal symmetry systems.
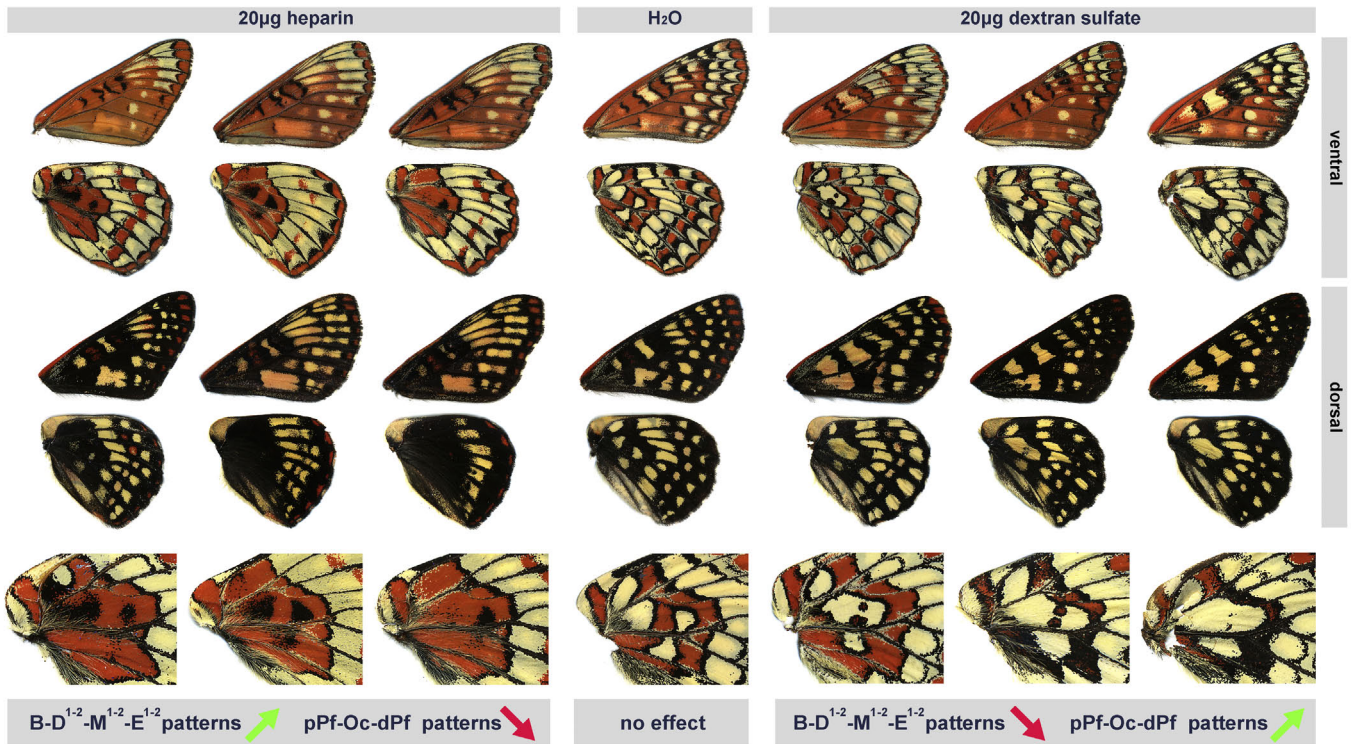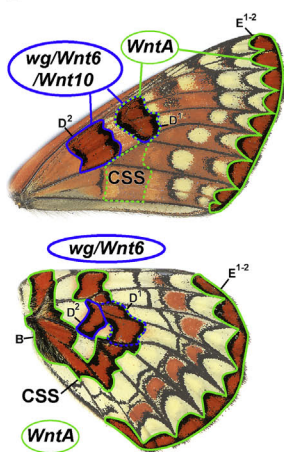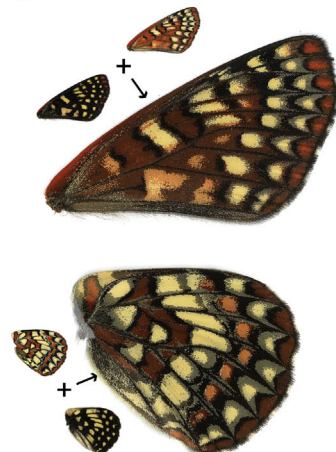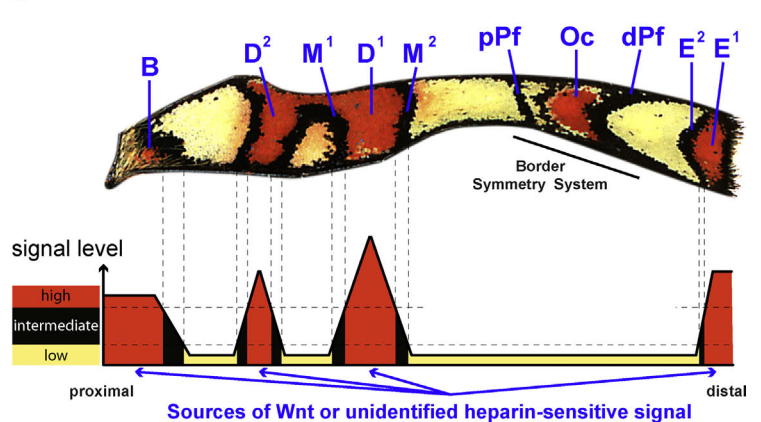
Fig. 3. Correlated distortions of *Wnt*-positive symmetry systems upon injection of sulfated polysaccharides. (A) Pattern distortions obtained by injections of heparin ($N=6$ individuals), dextran sulfate ($N=5$), and water ($N=3$) in early pupae of *E. chalcedona*. Multiple individuals representative of the observed range of variation are shown. Heparin and dextran sulfate have opposite effects on the size of *Wnt*-positive symmetry systems. (B) Summary of *Wnt* expression domains extrapolated on adult *E. chalcedona* ventral wings. *WntA* marks the basal, central (CSS) and external symmetry systems, while the *wg/Wnt6/Wnt10* cluster marks the D^2 and D^1 discal symmetry systems. (C) Superimposition of transparent ventral and dorsal sides of *E. chalcedona* wings. Black markings on the dorsal sides match the positions of nymphalid ground plan elements that are more readily identified on the ventral sides. (D) A morphogenetic model for the formation of the basal, discal, central, and external symmetry systems. The discrete deployment of sources of Wnt signals (and/or other heparin-sensitive morphogens) instructs pattern formation and concentration-dependent color boundaries along the proximo-distal axis. A section of the ventral hindwing (M^2–M^3 wing cell) illustrates the position of the *Wnt*-positive/heparin-sensitive symmetry systems.

Expression of WntA delineates the proximal contour of forewing white bands

While the buckeye butterfly *J. coenia* displays clear homologs of the *Euphydryas* B, D^{1-2}, Oc, and E^{1-2} patterns, it also shows a more divergent central symmetry system. On ventral hindwings, a pair of putative M^{1-2} stripes can be discerned from a homogenous background in summer-forms of this polyphenic butterfly. Only the M^1 band is visible on *J. coenia* forewings, and based on comparisons with closely related butterflies where the ground plan organization can be more readily interpreted (e.g. *Junonia lemonias*), M^1 corresponds to the proximal boundary of the white band that is widespread in this genus (Otaki, 2012). Expression of *WntA* in *J. coenia* wing disks showed a tripartite system of stripes (Fig. 4), similar in organization to the expression detected in *E. chalcedona*: (1) a basal expression domain marking the basal symmetry system; (2) a central expression domain; and (3) a marginal expression domain, possibly involved in the patterning of the E^{1-2} patterns. Of these, the central expression domain is particularly complex and bears further interpretation: In the hindwing, *WntA* expression is centered on a complete symmetry system, delimited by conspicuous M^1 and M^2 borders. In contrast,
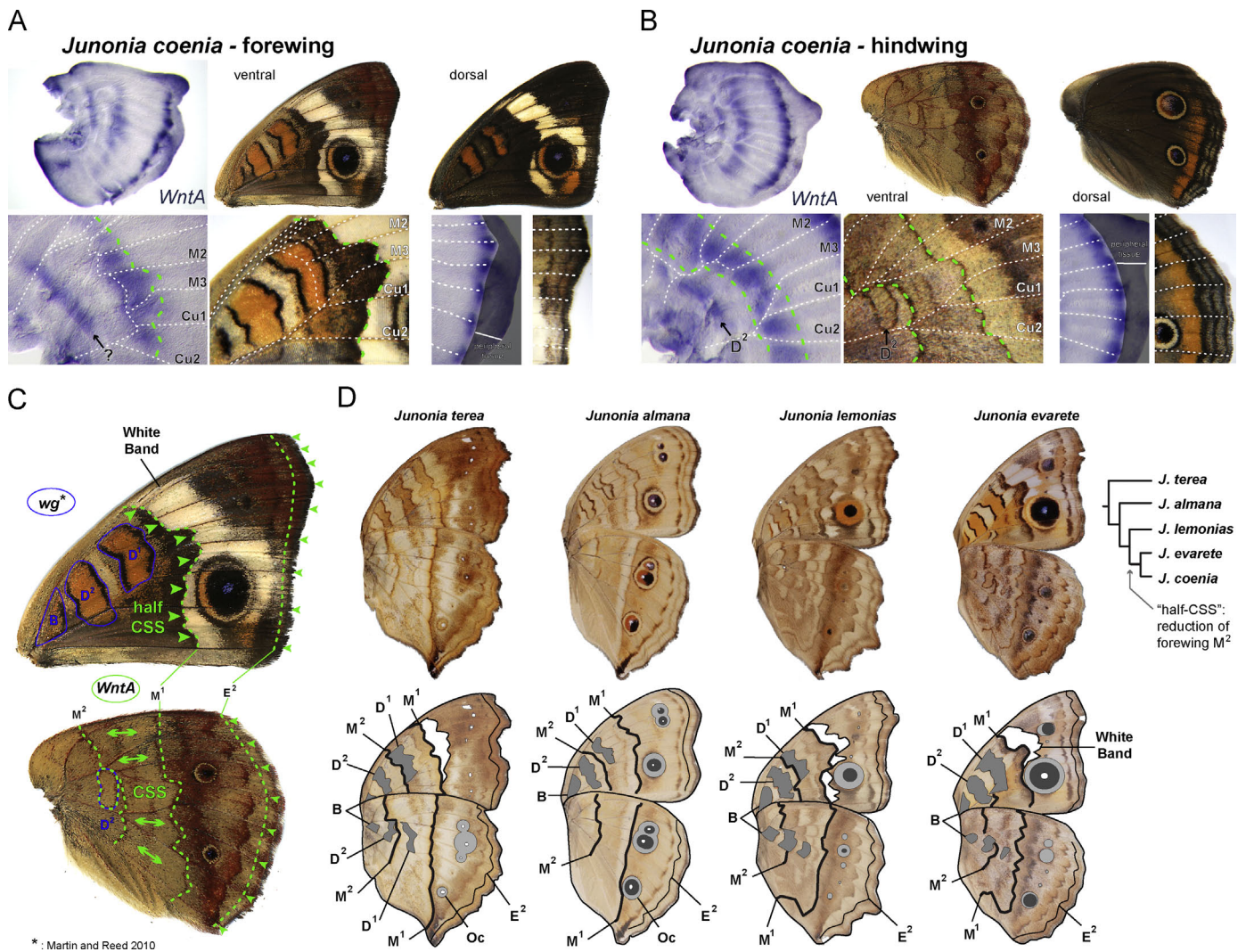
Fig. 4. Central expression of *WntA* in *J. coenia* marks the central symmetry system and delineates the forewing white band. (A) Expression of *WntA* in larval forewing disks of *J. coenia* (Stage 3.25). The distal edge of the central expression domain outlines the proximal contour of the white band (green dotted line). Question mark: expression domain possibly related to D^2 or to a cryptic pattern. (B) Expression of *WntA* in a larval hindwing disks of *J. coenia* (Stage 3.0). *WntA* marks the position of the central symmetry system, as seen by the spatial correspondence with the M^2 and M^1 boundaries (green dotted lines). (C) Summary of color pattern-related *Wnt* expression. *WntA* notably marks the central symmetry system (CSS) and is possibly associated with the external symmetry system; *wg* is expressed in the basal and discal symmetry systems (Martin and Reed, 2010). (D) Evolutionary derivations of the nymphalid ground plan in the genus *Junonia*. The lineage leading to *J. coenia* underwent a reduction of the forewing M^2 band. In addition, the proximal boundary of the white band visible in *J. coenia* forewings corresponds to a cryptic M^1 pattern, as revealed by more basal species. Tree topology is derived from a molecular phylogeny of the genus *Junonia* (Kodandaramaiah, 2009).

while *J. coenia* forewings appear more derived and lack an apparent central symmetry system, *WntA* still marks an elongated domain consistent in position with the existence of a functional central symmetry system. The distal border of this central *WntA* expression domain delimits the proximal shape and position of the forewing white band. Consistent with genetic evidence in *Limenitis* (Gallant et al., 2014), *WntA* may thus specify an active central symmetry system rendered cryptic by loss of symmetric organization (and loss of M^2). *WntA* expression in the forewings of both *Junonia* and *Limenitis* thus reveals a "half" central symmetry system with a functional M^1 border, which delineates the proximal contour of an immediately distal white band. These data provide strong evidence that the white bands of many nymphalid butterflies emerged by derivation of the M^1 boundary, as previously predicted in several analogous systems (Nijhout, 1991; Otaki, 2011; Schwanwitsch, 1935, 1956).

Of note, expression of *wg* has previously been described in the *J. coenia* B, D^1, and D^2 elements (Martin and Reed, 2010). Furthermore, heparin injections in *J. coenia* trigger pattern defects

(Serfas and Carroll, 2005) that, in the light of the expanded gene expression results here, can be interpreted as expansions of *Wnt*-positive patterns similar to our results in *E. chalcedona*. These data are consistent with a composite role of Wnt pathway genes in patterning various symmetry systems along the proximo-distal axis, but in contrast with *E. chalcedona*, *WntA*- and *wg*-associated patterns do not display the same color output in *J. coenia*, suggesting a greater degree of pattern individuation (see the section "Discussion").

Complex composite patterns: expression of WntA in V. cardui

The Painted Lady butterfly *V. cardui* shows intricate color patterns in basal and median wing regions that resist confident association with the nymphalid ground plan. We thus sought to use this species to test the potential of *WntA* expression to clarify homology relationships in complex patterns (Fig. 5). Intense expression of *WntA* roughly replicated the tripartite expression of *WntA* into basal, median, and external patterns, but correlations
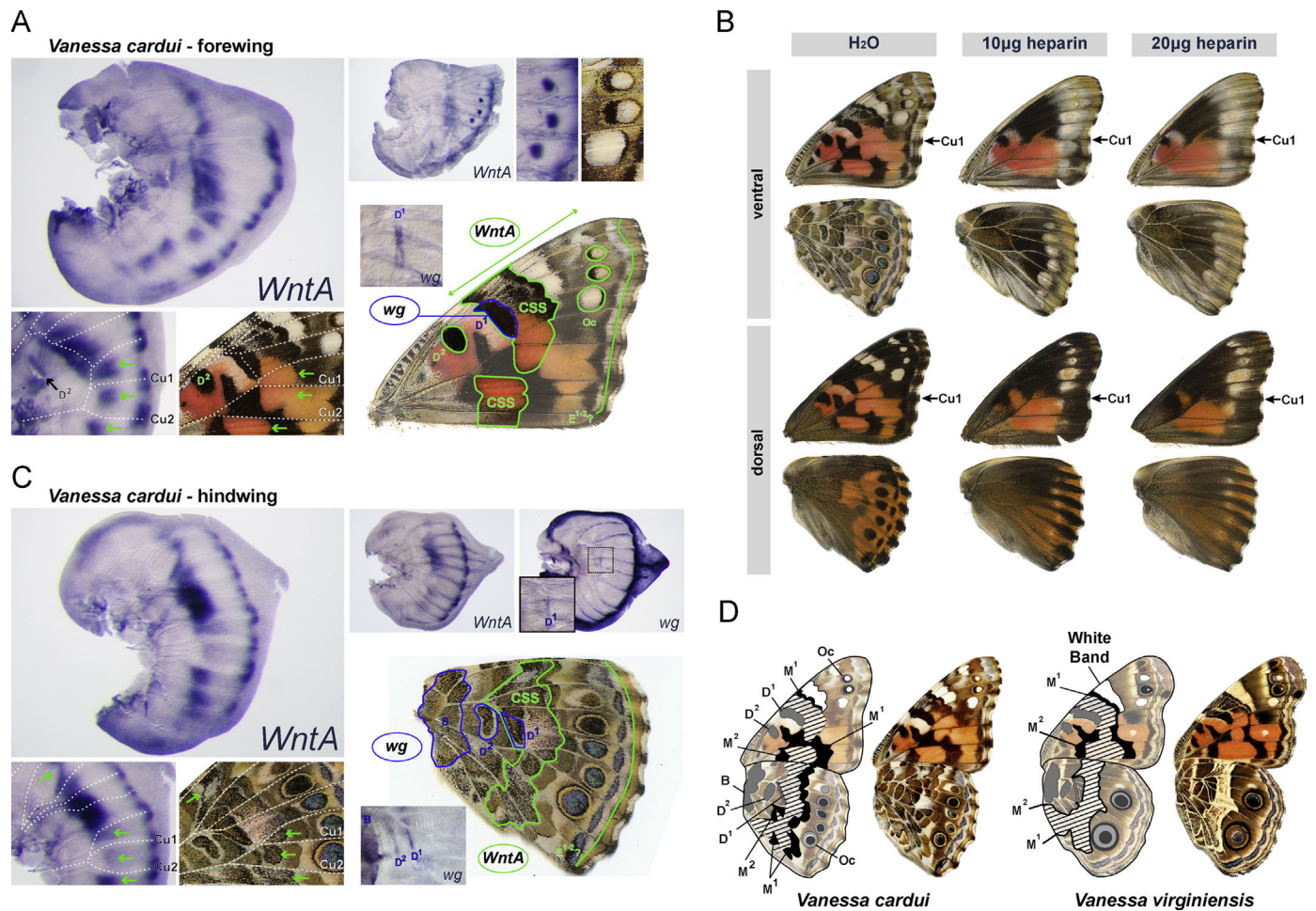
Fig. 5. *WntA* expression in the complex patterns of *V. cardui*. (A) Expression of Wnt ligands in the larval forewing disks of *V. cardui* (left: Stage 2.25; top right Stage 3.75). *WntA* is expressed in D^2, along an antero-posterior stripe correlating with boundaries of the central symmetry system (CSS, green arrows), in the external symmetry system, and becomes expressed in the presumptive forewing eyespots at late stages (upper panels). Notice the discontinuous expression of *WntA* in the Cu1–Cu2 vein compartment. *wg* is expressed in D^1 (inset: Stage 3.0). (B) Heparin injections result in distinct effects on color composition anterior and posterior to the forewing Cu1 vein (see text for details). (C) Expression of *Wnt* ligand genes in larval hindwing disks. *WntA* is expressed in an antero-posterior stripe that correlates with a complex central symmetry system (CSS; left: Stage 2.0; top center – *WntA*: Stage 3.25; top right – *wg*: Stage 3.25). Notice the pattern correspondences in wing cells with well-marked pattern boundaries (green arrows). *WntA* is also expressed along the wing margin, most likely marking the external symmetry system. *wg* is expressed in D^1 (top right panel) and later gains expression in B and D^2 (bottom inset – *wg*: Stage 3.75). (D) Inferred *V. cardui* nymphalid ground plan patterns homologized to presumptive ground plan elements in the closely related species *V. virginiensis*. Hashed domain denotes the inferred central expression of *WntA*. Notice the continuous M^1 band in *V. virginiensis* forewings.

with adult morphology were not immediately obvious to the naked eye. The relative position of *WntA* expression and vein intersections suggests that *WntA* implies a functional symmetry system in both the forewing and hindwing.

In the anterior half of the forewing (anterior to the Cu1 vein), *WntA* may pattern the limits of a gray/black symmetric field between the discal spot and a white band, a view that is supported by the sweeping effect of heparin injections, which expand the distribution of black color in that region (Fig. 5A and B). In the posterior forewing (posterior to the Cu1 vein), *WntA* expression corresponds to patches of orange color outlined of black. Interestingly, heparin injections reveal a dual effect across the antero-posterior axis of the forewing: in contrast with the expansion of black color in the wing cells anterior to the Cu1 vein, orange color expands in the posterior compartment. We note that the central symmetry system can be readily extrapolated from the simpler forewings of the related species *Vanessa virginiensis*: in this species, the central system forms an uninterrupted stripe that shifts from black/gray (anterior to Cu1) to orange (posterior to Cu1). We interpret that this antero-posteriorly subdivided nature of the central symmetry system is conserved in *V. cardui*, which differs by a dislocation of the orange stripe at the level of the Cu1

vein, reflected by the discontinuous expression of *WntA* in the Cu1-2 compartment (Fig. 5A).

In the ventral hindwing, *WntA* medial expression suggests a role in the specification of a central symmetry system, although its exact boundaries are obscured by the complexity of successive color waves in the adult color patterns (Fig. 5C). The presence of a central symmetry system in this genus is more conspicuous in *V. virginiensis*, and we deduce that *V. cardui* represents a derived state that illustrates the tendency of the central symmetry system to depart from the ground plan morphology. In addition, the position of the B, D^1, and D^2 patterns correlates with expression of *wg*, in both forewings and hindwings dissected at the latest stages obtained [> 3.25 in the reference staging system (Reed et al., 2007)]. These results suggest that the various Wnt signaling genes can trigger different color outputs across different regions of the wing, thus adding to the complexity of color patterns in *V. cardui*. It is challenging in some respects, however, to interpret the effects of heparin in light of *WntA* expression, because treated hindwings display homogenous fields of central black scales that make it difficult to identify specific pattern expansions (Fig. 5B). The modulating effects of heparin-like sugar chains are not exclusive to Wnt ligands and have been linked to the movement

of other signaling molecules of the Hedgehog, TGF-β, and FGF families (Lin, 2004; Yan and Lin, 2009). Due to the weaker correlation between heparin and *Wnt* expression data in *V. cardui*, it is possible that heparin interacts with other patterning signals that are yet to be identified in this species, and that may possibly contribute to the complexity of its color pattern organization.

Finally, we were surprised to observe *WntA* expression in the presumptive forewing eyespots – expression only visible at the latest stages of fifth instar forewing disk development (> Stage 3.0). This expression was neither observed in the hindwing eyespots from the same individuals nor in the eyespots of other species. While nymphalid eyespots are considered to be homologous features, they also show heterogeneity in the set of developmental genes they express or in their timing of expression (Oliver et al., 2012; Shirai et al., 2012). The observation of *WntA* expression in *V. cardui* eyespots may thus reflect: (1) a recent co-option of *WntA* into the formation of forewing eyespots; (2) an ancient co-option followed by extensive loss of expression in many lineages; or (3) a heterochronic shift, from a yet to be observed pupal eyespot expression to a late larval expression. In any case, *WntA* is a new addition to the set of known eyespot genes and may contribute to the diversity of these patterns elements.

Expression of WntA in A. vanillae reveals a dislocated central symmetry system

A complex set of silver color patches with a black outline ornaments the ventral side of the Gulf Fritillary butterfly *A. vanillae*. While these patterns defy unambiguous affiliation to specific elements of the nymphalid ground plan, Nijhout and Wray previously suggested that spot patterns in basal heliconiine butterflies such as *A. vanillae* represent a dislocation of the M^1 and M^2 bands (Nijhout and Wray, 1988). Here, we validate this prediction by showing that *WntA* expression uncovers many small, distinct expression domains in the *A. vanillae* wing, contrasting with the continuous or aligned expression patterns of *WntA* in other species assessed so far. Each spot of *WntA* expression corresponds to an adult pattern (silver spots on the ventral surface, black spots on the dorsal surface). In addition, this complex deployment of *WntA* is complemented by expression of *wg* in D^2 (*WntA*-negative) and D^1 (*WntA*-positive). All the *Wnt*-positive patterns showed a dramatic expansion upon heparin injection, and conversely, silver spots for which we could not detect *wg* or *WntA* expression contracted or disappeared upon heparin treatment, suggesting a different developmental and evolutionary origin. In other words, both gene expression and heparin injections converge to provide evidence that the Wnt pathway specifies most silver spot patterns in *A. vanillae*, with *WntA* notably marking dislocated elements that diverged from the ground plan organization.

Discussion

Derivations of the central symmetry system: a review of previous predictions

The central symmetry system is an important and dynamic component of butterfly wing patterns, and previous literature has attempted to identify this structure across a broad range of species by comparing adult morphologies (Nijhout, 1991; Otaki, 2012; Schwanwitsch, 1924, 1956; Süffert, 1927) (Fig. 1B–G). More recent reevaluation of this work has resulted in a developmental theory explaining the formation and evolution of butterfly wing symmetry systems (Nijhout, 1994, 2001). We highlight here a few of its axioms:

A. By definition, the central symmetry system shows axial symmetry in its ground plan state, with M^1 and M^2 representing the outmost, similarly colored pigment bands. To explain this symmetric organization, it has been proposed that the central symmetry system is patterned by signaling molecules expressed along its central axis of symmetry (Nijhout, 1978, 1994; Toussaint and French, 1988).
B. M^1 and M^2 often share an identical color composition with the D^1 and D^2 elements (e.g., Fig. 1C, F–G). This similarity suggests a shared developmental basis between these symmetry systems.
C. Absence of M^2, the proximal band of the central symmetry system, is a common theme of nymphalid evolution. Nijhout referred to this pattern variant as a "half symmetry system" (Nijhout, 1991). In these cases, the loss of axial symmetry makes it challenging to identify the central symmetry system, but color pattern boundaries that run from the anterior to posterior borders of the wings in the central region are often assigned as homologs of the M^1 counterpart of the symmetry system (Nijhout, 1991).
D. In many nymphalids, the central symmetry system shows dislocation effects between vein-defined compartments (e.g., Fig. 1G), resulting in a slippage effect resembling "geological faultlines" (Nijhout, 2001). In extreme cases, these bands form individualized spot-like patterns devoid of obvious alignment on the antero-posterior axis. It was suggested that dislocated patterns would result from similarly discontinuous sources of organizing molecules during development (Nijhout, 1994).

Overall, however, ambiguous homology relationships and absence of developmental data have impeded conclusive comparisons between species, and therefore many homology predictions have remained untested hypotheses. Here we used *WntA* expression as a marker of the central symmetry system to assess several cases of color pattern homology using developmental data.

WntA and wg/Wnt6/Wnt10 are putative organizers of distinct nymphalid symmetry systems

The mirror-like organization of symmetry systems has been proposed to derive from gradients of extracellular substances, expressed along axes of symmetry, that induce color fate in a concentration-dependent manner. Here we found that several Wnt ligands are expressed in these predicted signaling centers during wing disk development, consistent with a direct role for Wnts in the organization of color patterns. Indeed, Wnt proteins are extracellular signaling ligands known to be involved in the deployment of positional information in developing tissues, and the Wnt gene *wg* has been shown to specify pigment patterns in *Drosophila* wings (Werner et al., 2010). Importantly, the evidence that the Wnt pathway plays an active role in butterfly wing patterning is more than circumstantial in spite of the difficulty to conduct transgenic experiments: genetic mapping of natural phenotypic variation has independently pinpointed a causal role for *WntA* in two clades of *Heliconius* butterflies as well as in *L. arthemis* (Gallant et al., 2014; Martin et al., 2012; Nadeau et al., 2014; Papa et al., 2013). While we presently lack the tools to assess if Wnt ligands are alone sufficient to trigger pattern formation, or if they are alone responsible for inductive gradients, the replicated finding that Wnt expression correlates with the symmetry centers of many patterns is strongly indicative of a direct role in pattern specification, particularly in the context of previous genetic mapping and association work.

WntA is the first gene associated with the central symmetry system, filling in a major piece of the nymphalid ground plan puzzle that was previously missing from developmental studies. In *E. chalcedona*, where the ground plan configuration is best visible on the ventral hindwing, *WntA* prefigures the position of basal,

discal, central, and external symmetry patterns of identical color composition. This set of orange and black patterns is completed by expression of *wg* in the D patterns, as previously described in other lepidopterans (Martin and Reed, 2010), as well as *Wnt6* and *Wnt10*. Only Wnt-positive patterns expand upon heparin treatment, consistent with prior work showing that heparin enhances Wnt signals. Overall, the picture emerging from the relatively simple *E. chalcedona* wing pattern highlights Wnt ligands as the organizers of all described symmetry systems except the border symmetry system.

Individuation and reduction of the symmetry systems

While for a given nymphalid species, we can often expect a similar color composition among seemingly *Wnt*-positive patterns such as the discal, central, and external symmetry systems (e.g., Fig. 1C and D, G and H), other butterflies show an uncoupling between these distinct pattern sets. For instance, *wg*-positive discal symmetry systems are orange with a black outline in *J. coenia* and *L. arthemis* (Martin and Reed, 2010), while *WntA* expression does not correlate with such colors in these species (Gallant et al., 2014) (Fig. 4). Importantly, we notice that certain *Junonia* species (e.g., *Junonia terea*) present a less derived wing pattern organization which, as in *E. chalcedona*, show a complete central symmetry system with both M^{1-2} bands framing a mirror-like color field, and similar color compositions between *Wnt*-positive patterns such as the discal and central symmetry systems. We thus conclude that *J. coenia* represents an example of pattern individuation and reduction that has diverged from the ground plan organization, resulting in a loss of the M^{1-2} symmetric color field (orange outlined by black in *J. terea*), followed by a reduction of the M^1 band itself, still visible as a black line in some *J. coenia*

populations or in closely related species such as *Junonia evarete* (Fig. 4D). However, a vestigial form of the central symmetry system persists in *J. coenia*, with central *WntA* expression delineating the immediately distal forewing white band. A similar scenario may have taken place in the Limenitidinae clade, where *WntA* alleles determine white band presence/absence in *L. arthemis* (Gallant et al., 2014). Indeed, extant representatives of the nymphalid ground plan configuration in Limenitidinae such as *Euryphura* and *Bebearia* suggest that the central system has undergone a secondary loss of its symmetric organization in the lineage leading to *Limenitis*. Both the genus *Junonia* and the subfamily Limenitidinae thus provide independent replicates of pattern evolution where the central symmetry system has undergone parallel reductions. In the most derived forms of both clades, *WntA* specifies a cryptic M^1 band that corresponds to the proximal boundary of the white band. Together, these results highlight the utility of gene expression patterns to establish homology relationships between characters that have long diverged morphologically.

Antero-posterior subcompartmentalization of central symmetry systems

In addition to its modifications on the proximo-distal axis, the central symmetry system has also deviated along the antero-posterior axis by breaking its original expression as a continuous stripe. A first example is visible in the ventral forewing of *V. cardui*, where the color outputs of the *WntA*-positive fields differ between the anterior and posterior compartments, as delimited by the Cu1 vein (Fig. 5A). This dual nature of the *V. cardui* central symmetry system is supported by heparin injections, which resulted in an expansion of black color anterior to Cu1 and in an expansion of orange/pink color posterior to Cu1. Developmental factors that
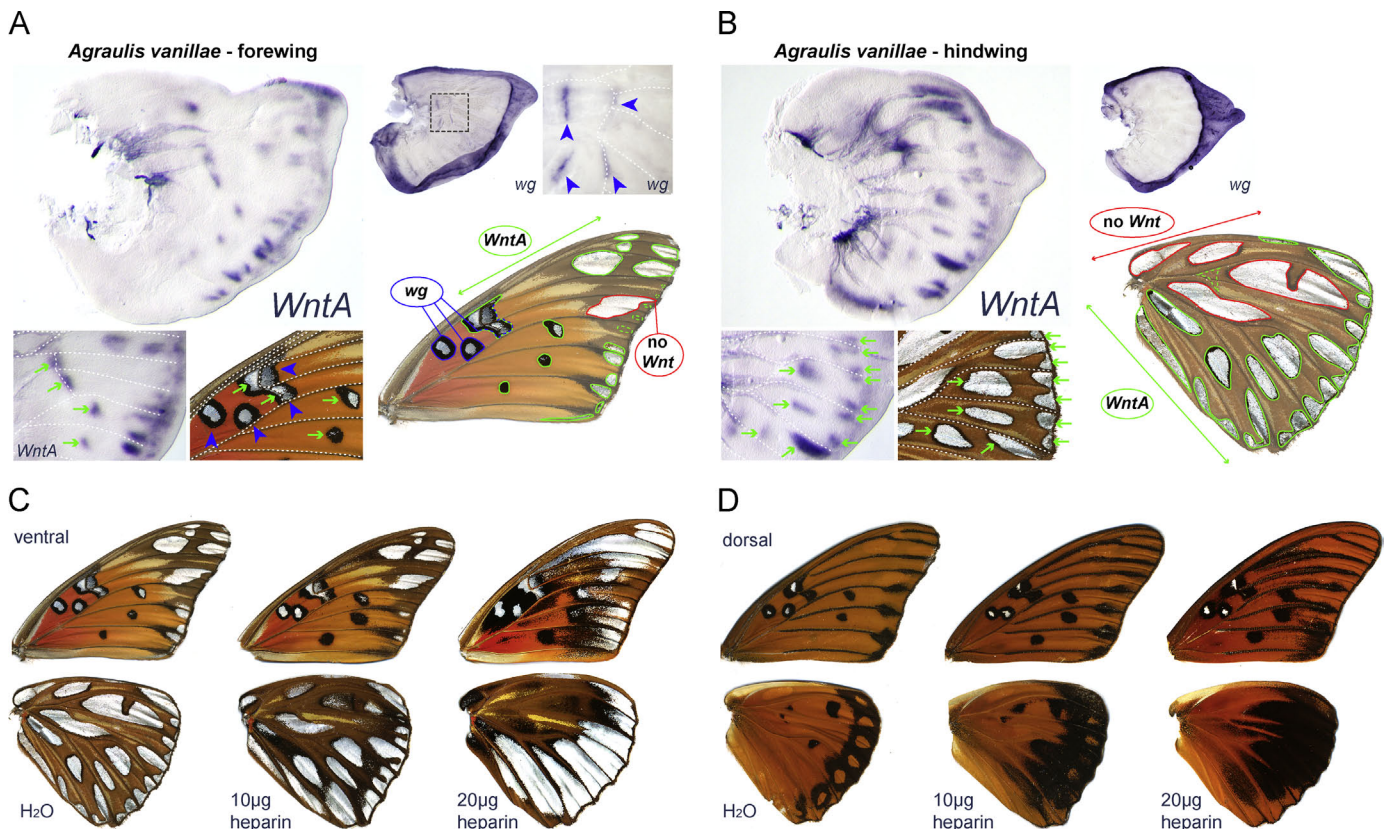

Fig. 6. Dislocated expression of *Wnt* patterns in *A. vanillae*. Expression of *WntA* (green arrows and lines) and *wg* (blue arrowheads and lines) mark presumptive silver spots across the (A) forewing imaginal disks (left – *WntA*: Stage 2.0; top right – *wg*: Stage 3.25) and (B) hindwing imaginal disks (left – *WntA*: Stage 2.0; top right – *wg*: Stage 3.25). (C) Heparin injections result in expansion of *Wnt*-positive patterns and reduction or loss of *Wnt*-negative patterns.

organize the antero-posterior axis of the wing may thus act concomitantly with *WntA* or downstream of it, triggering an uncoupling of color patterning in two different wing compartments.

The second example illustrates the tendency of symmetry systems to dislocate at the level of wing veins, a phenomenon that has been well documented in many lepidopterans (Nijhout, 1978, 1994, 2001). This pattern dislocation effect is visible in *A. vanillae*, as revealed by the dispersed expression of *WntA* (Fig. 6). We speculate that signals involved in vein positioning and expressed in the vein field have become local inhibitors of *WntA* transcription. This could explain how *WntA* is expressed at equidistance from bordering veins in this species – with the discal crossvein (D^1 pattern) as an exception. In other words, *WntA* highlights the homology of certain dislocated patterns with the central symmetry system, indicating how morphological diversification may have followed a few simple principles.

Conclusion

Wnt ligands provide positional information across undifferentiated tissues and play key roles in the development of organized structures throughout the animal kingdom. Because evolution of form involves the repeated use of genes specialized in development (Carroll et al., 2004), signaling genes specialized for tissue patterning are likely to host the genetic variation that underlies morphological diversity. An experimental validation of this hypothesis has emerged from studies that mapped the genetic basis of butterfly wing pattern variation to *WntA*. Importantly, genetic evolution of *WntA* itself has repeatedly driven pattern shifts in distinct lineages (Gallant et al., 2014; Martin et al., 2012), implying a predictable genetic basis for the evolution of these phenotypic traits (Martin and Orgogozo, 2013; Papa et al., 2008). Here we have extended the generality of this finding to deeper phylogenetic levels, with *WntA* expression clarifying homology relationships between derived patterns across the family Nymphalidae. Our data suggest that the spatial control of *WntA* expression, via *cis*-regulatory evolution or by modification of upstream regulators, has been a major mechanism repeatedly driving variation in color pattern position and shape. Butterfly wings thus form a mosaic of evolutionary characters where complex changes can be decomposed into relatively simple mechanisms that occur early during wing development. In this system, the foundations of intra-specific change that have been identified in natural populations may generally extend to macro-evolutionary levels, thus encouraging evolutionary comparisons that encompass very different time scales (Kopp, 2009; Muller, 2007; Nunes et al., 2013; Pigliucci and Müller, 2010).

Acknowledgments

Appendix A. Supporting information

Supplementary data associated with this article can be found in the online version at http://dx.doi.org/10.1016/j.ydbio.2014.08.031.

References

Baeg, G.H., Lin, X., Khare, N., Baumgartner, S., Perrimon, N., 2001. Heparan sulfate proteoglycans are critical for the organization of the extracellular distribution of Wingless. Development 128, 87–94.

Beldade, P., Brakefield, P.M., 2002. The genetics and evo-devo of butterfly wing patterns. Nat. Rev. Genet. 3, 442–452.

Beldade, P., Saenko, S.V., 2009. Evolutionary and developmental genetics of butterfly wing patterns: focus on Bicyclus anynana eyespots. In: Goldsmith, M.R., Marec, F. (Eds.), Molecular Biology and Genetics of the Lepidoptera (Contemporary Topics in Entomology). CRC Press, Boca Raton, pp. 89–104.

Binari, R.C., Staveley, B.E., Johnson, W.A., Godavarti, R., Sasisekharan, R., Manoukian, A.S., 1997. Genetic evidence that heparin-like glycosaminoglycans are involved in wingless signaling. Development 124, 2623–2632.

Bolognesi, R., Beermann, A., Farzana, L., Wittkopp, N., Lutz, R., Balavoine, G., Brown, S.J., Schroder, R., 2008. Tribolium Wnts: evidence for a larger repertoire in insects with overlapping expression patterns that suggest multiple redundant functions in embryogenesis. Dev. Genes Evol. 218, 193–202.

Bradley, R.S., Brown, A.M., 1990. The proto-oncogene int-1 encodes a secreted protein associated with the extracellular matrix. EMBO J. 9, 1569.

Brunetti, C.R., Selegue, J.E., Monteiro, A., French, V., Brakefield, P.M., Carroll, S.B., 2001. The generation and diversification of butterfly eyespot color patterns. Curr. Biol. 11, 1578–1585.

Carroll, S.B., Gates, J., Keys, D.N., Paddock, S.W., Panganiban, G.E., Selegue, J.E., Williams, J.A., 1994. Pattern formation and eyespot determination in butterfly wings. Science 265, 109–114.

Carroll, S.B., Grenier, J.K., Weatherbee, S.D., 2004. From DNA to Diversity: Molecular Genetics and the Evolution of Animal Design. Blackwell Science, Malden, MA.

Dohrmann, C.E., Nijhout, H.F., 1988. Development of the wing margin in *Precis coenia* (Lepidoptera: Nymphalidae). J. Res. Lepid. 27, 151–159.

Floer, M., Götte, M., Wild, M.K., Heidemann, J., Gassar, E.S., Domschke, W., Kiesel, L., Luegering, A., Kucharzik, T., 2010. Enoxaparin improves the course of dextran sodium sulfate-induced colitis in syndecan-1-deficient mice. Am. J. Pathol. 176, 146–157.

Fuerer, C., Habib, S.J., Nusse, R., 2010. A study on the interactions between heparan sulfate proteoglycans and Wnt proteins. Dev. Dyn. 239, 184–190.

Gallant, J.R., Imhoff, V.E., Martin, A., Savage, W.K., Chamberlain, N.L., Pote, B.L., Peterson, C., Smith, G.E., Evans, B., Reed, R.D., et al., 2014. Ancient homology underlies adaptive mimetic diversity across butterflies. Nat. Commun. 5 (http://dx.doi.org/10.1038/ncomms5817).

Gieseler, K., Wilder, E., Mariol, M.-C., Buratovich, M., Bérenger, H., Graba, Y., Pradel, J., 2001. DWnt4 and wingless elicit similar cellular responses during imaginal development. Dev. Biol. 232, 339–350.

Greco, V., Hannus, M., Eaton, S., 2001. Argosomes: a potential vehicle for the spread of morphogens through epithelia. Cell 106, 633–645.

Heliconius Genome Consortium, 2012. Butterfly genome reveals promiscuous exchange of mimicry adaptations among species. Nature 487, 94–98.

Hogvall, M., Schonauer, A., Budd, G., McGregor, A., Posnien, N., Janssen, R., 2014. Analysis of the Wnt gene repertoire in an onychophoran provides new insights into the evolution of segmentation. EvoDevo 5, 14.

Hufnagel, L., Kreuger, J., Cohen, S.M., Shraiman, B.I., 2006. On the role of glypicans in the process of morphogen gradient formation. Dev. Biol. 300, 512–522.

Janson, K., Cohen, E.D., Wilder, E.L., 2001. Expression of DWnt6, DWnt10, and DFz4 during Drosophila development. Mech. Dev. 103, 117–120.

Janssen, R., Le Gouar, M., Pechmann, M., Poulin, F., Bolognesi, R., Schwager, E., Hopfen, C., Colbourne, J., Budd, G., Brown, S., et al., 2010. Conservation, loss, and redeployment of Wnt ligands in protostomes: implications for understanding the evolution of segment formation. BMC Evol. Biol. 10, 374.

Joron, M., Jiggins, C.D., Papanicolaou, A., McMillan, W.O., 2006. Heliconius wing patterns: an evo-devo model for understanding phenotypic diversity. Heredity 97, 157–167.

Joron, M., Frezal, L., Jones, R.T., 2011. Chromosomal rearrangements maintain a polymorphic supergene controlling butterfly mimicry. Nature 477, 203–206.

Kodandaramaiah, U., 2009. Eyespot evolution: phylogenetic insights from Junonia and related butterfly genera (Nymphalidae: Junoniini). Evol. Dev. 11, 489–497.

Kopp, A., 2009. Metamodels and phylogenetic replication: a systematic approach to the evolution of developmental pathways. Evolution 63, 2771–2789.

Kunte, K., Zhang, W., Tenger-Trolander, A., Palmer, D.H., Martin, A., Reed, R.D., Mullen, S.P., Kronforst, M.R., 2014. doublesex is a mimicry supergene. Nature 507, 229–232.

Lin, X., 2004. Functions of heparan sulfate proteoglycans in cell signaling during development. Development 131, 6009–6021.

Macdonald, W.P., Martin, A., Reed, R.D., 2010. Butterfly wings shaped by a molecular cookie cutter: evolutionary radiation of lepidopteran wing shapes associated with a derived Cut/wingless wing margin boundary system. Evol. Dev. 12, 296–304.

Martin, A., Orgogozo, V., 2013. The loci of repeated evolution: a catalog of genetic hotspots of phenotypic variation. Evolution 67, 1235–1250.

Martin, A., Reed, R.D., 2010. wingless and aristaless2 define a developmental ground plan for moth and butterfly wing pattern evolution. Mol. Biol. Evol. 27, 2864–2878.

Martin, A., Papa, R., Nadeau, N.J., Hill, R.I., Counterman, B.A., Halder, G., Jiggins, C.D., Kronforst, M.R., Long, A.D., McMillan, W.O., et al., 2012. Diversification of complex butterfly wing patterns by repeated regulatory evolution of a Wnt ligand. Proc. Natl. Acad. Sci. 109, 12632–12637.

Monteiro, A., French, V., Smit, G., Brakefield, P.M., Metz, J., 2001. Butterfly eyespot patterns: evidence for specification by a morphogen diffusion gradient. Acta Biother. 49, 77–88.

Muller, G.B., 2007. Evo-devo: extending the evolutionary synthesis. Nat. Rev. Genet. 8, 943–949.

Nadeau, N., Ruiz, M., Salazar, P., Counterman, B., Medina, J.A., Ortiz-Zuazaga, H., Morrison, A., McMillan, W.O., Jiggins, C.D., Papa, R., 2014. Population genomics of parallel hybrid zones in the mimetic butterflies, *H. melpomene* and *H. erato*. Genome Res. (http://dx.doi.org/10.1101/gr.169292.113).

Nijhout, H.F., 1978. Wing pattern formation in Lepidoptera: a model. J. Exp. Zool. 206, 119–136.

Nijhout, H.F., 1980. Pattern formation on lepidopteran wings: determination of an eyespot. Dev. Biol. 80, 267–274.

Nijhout, H.F., 1985. Cautery-induced colour patterns in *Precis coenia* (Lepidoptera: Nymphalidae). J. Embryol. Exp. Morphol. 86, 191–203.

Nijhout, H.F., 1991. The Development and Evolution of Butterfly Wing Patterns. Smithsonian Institution Press, Washington, DC.

Nijhout, H.F., 1994. Symmetry systems and compartments in Lepidopteran wings: the evolution of a patterning mechanism. Development 1994, 225–233.

Nijhout, H.F., 2001. Elements of butterfly wing patterns. J. Exp. Zool. 291, 213–225.

Nijhout, H.F., Wray, G.A., 1988. Homologies in the colour patterns of the genus Heliconius (Lepidoptera: Nymphalidae). Biol. J. Linn. Soc. 33, 345–365.

Nunes, M.D.S., Arif, S., Schlötterer, C., McGregor, A.P., 2013. A perspective on micro-evo-devo: progress and potential. Genetics 195, 625–634.

Oliver, J.C., Tong, X.-L., Gall, L.F., Piel, W.H., Monteiro, A., 2012. A Single origin for nymphalid butterfly eyespots followed by widespread loss of associated gene expression. PLoS Genet. 8, e1002893.

Otaki, J.M., 2011. Color-pattern analysis of eyespots in butterfly wings: a critical examination of morphogen gradient models. Zool. Sci. 28, 403–413.

Otaki, J.M., 2012. Color pattern analysis of nymphalid butterfly wings: revision of the Nymphalid groundplan. Zool. Sci. 29, 568–576.

Papa, R., Martin, A., Reed, R.D., 2008. Genomic hotspots of adaptation in butterfly wing pattern evolution. Curr. Opin. Genet. Dev. 18, 559–564.

Papa, R., Kapan, D.D., Counterman, B.A., Maldonado, K., Lindstrom, D.P., Reed, R.D., Nijhout, H.F., Hrbek, T., McMillan, W.O., 2013. Multi-allelic major effect genes interact with minor effect QTLs to control adaptive color pattern variation in *Heliconius erato*. PLoS One 8, e57033.

Pigliucci, M., Müller, G.B., 2010. Evolution – The Extended Synthesis. The MIT Press, Cambridge, MA.

Reed, R.D., Serfas, M.S., 2004. Butterfly wing pattern evolution is associated with changes in a Notch/Distaless temporal pattern formation process. Curr. Biol. 14, 1159–1166.

Reed, R.D., Chen, P.H., Nijhout, H.F., 2007. Cryptic variation in butterfly eyespot development: the importance of sample size in gene expression studies. Evol. Dev. 9, 2–9.

Reed, R.D., Papa, R., Martin, A., Hines, H.M., Counterman, B.A., Pardo-Diaz, C., Jiggins, C.D., Chamberlain, N.L., Kronforst, M.R., Chen, R., et al., 2011. optix drives the repeated convergent evolution of butterfly wing pattern mimicry. Science 333, 1137–1141.

Reichsman, F., Smith, L., Cumberledge, S., 1996. Glycosaminoglycans can modulate extracellular localization of the wingless protein and promote signal transduction. J. Cell Biol. 135, 819–827.

Saenko, S., Marialva, M., Beldade, P., 2011. Involvement of the conserved Hox gene Antennapedia in the development and evolution of a novel trait. EvoDevo 2, 9.

Schwanwitsch, B.N., 1924. On the groundplan of the wing pattern in nymphalids and certain other families of rhopalocerous Lepidoptera. Proc. Zool. Soc. Lond. 34, 509–528.

Schwanwitsch, B.N., 1935. Evolution of the wing-pattern in palaearctic Satyridae. III. Genus Pararge and five others. Acta Zool. 16, 145–281.

Schwanwitsch, B.N., 1956. Color-pattern in Lepidoptera. Entomol. Obozr. 35, 530–546.

Serfas, M.S., Carroll, S.B., 2005. Pharmacologic approaches to butterfly wing patterning: sulfated polysaccharides mimic or antagonize cold shock and alter the interpretation of gradients of positional information. Dev. Biol. 287, 416–424.

Shirai, L., Saenko, S., Keller, R., Jeronimo, M., Brakefield, P., Descimon, H., Wahlberg, N., Beldade, P., 2012. Evolutionary history of the recruitment of conserved developmental genes in association to the formation and diversification of a novel trait. BMC Evol. Biol. 12, 21.

Süffert, F., 1927. Zur vergleichenden Analyse der Schmetterlingszeichnung. Biol. Zentralbl. 47, 385–413.

Süffert, F., 1929. Morphologische Erscheinungsgruppen in der Flugelzeichnung der Schmetterlinge, insbesondere die Querbindenzeichnung. Wilhelm Roux Arch. Entwicklungsmech. Org. 120, 299–353.

Toussaint, N., French, V., 1988. The formation of pattern on the wing of the moth, *Ephestia kuhniella*. Development 103, 707–718.

Werner, T., Koshikawa, S., Williams, T.M., Carroll, S.B., 2010. Generation of a novel wing colour pattern by the Wingless morphogen. Nature 464, 1143–1148.

Yan, D., Lin, X., 2009. Shaping morphogen gradients by proteoglycans. Cold Spring Harb. Perspect. Biol. 1, a002493.

Zhan, S., Reppert, S.M., 2013. MonarchBase: the monarch butterfly genome database. Nucleic Acids Res. 41 (Database issue), D758–D763 http://dx.doi.org/10.1093/nar/gks1057)2012.